

Article

Non-Antibiotic Antimony-Based Antimicrobials

Nikolay Gerasimchuk ^{1,*}, Kevin Pinks ¹, Tarosha Salpadoru ², Kaitlyn Cotton ², Olga Michka ², Marianna A. Patrauchan ^{2,*} and Karen L. Wozniak ²

¹ Department of Chemistry and Biochemistry, Temple Hall 456, Missouri State University, Springfield, MO 65897, USA

² Department of Microbiology and Molecular Genetics, Oklahoma State University, Stillwater, OK 74078, USA

* Correspondence: nngerasimchuk@missouristate.edu (N.G.); m.patrauchan@okstate.edu (M.A.P.); Tel.: +1-(417)-836-5165 (N.G.); +1-(405)-744-8148 (M.A.P.)

Abstract: A series of the eight novel organoantimony(V) cyanoximates of $\text{Sb}(\text{C}_6\text{H}_5)_4\text{L}$ composition was synthesized using the high-yield heterogeneous metathesis reaction between solid AgL (or TIL) and $\text{Sb}(\text{C}_6\text{H}_5)_4\text{Br}$ in CH_3CN at room temperature. Cyanoximes L were specially selected from a large group of 48 known compounds of this subclass of oximes on the basis of their water solubility and history of prior biological activity. The synthesized compounds are well soluble in organic solvents and were studied using a variety of conventional spectroscopic and physical methods. The crystal structures of all reported organometallic compounds were determined and revealed the formation of the distorted trigonal bipyramidal environment of the Sb atom and monodentate axial binding of acido-ligands via the O atom of the oxime group. The compounds are thermally stable in the solid state and in solution molecular compounds. For the first time, this specially designed series of organoantimony(V) compounds is investigated as potential non-antibiotic antimicrobial agents against three bacterial and two fungal human pathogens known for their increasing antimicrobial resistance. Bacterial pathogens included Gram-negative *Escherichia coli* and *Pseudomonas aeruginosa*, and Gram-positive *Staphylococcus aureus*. Fungal pathogens included *Cryptococcus neoformans* and *Candida albicans*. The cyanoximates alone showed no antimicrobial impact, and the incorporation of the SbPh_4 group enabled the antimicrobial effect. Overall, the new antimony compounds showed a strong potential as both broad- and narrow-spectrum antimicrobials against selected bacterial and fungal pathogens and provide insights for further synthetic modifications of the compounds to increase their activities.

Keywords: cyanoximes; organometallic compounds of antimony(V); crystal structures; antimicrobial activity; antibacterial activity; antifungal activity



Citation: Gerasimchuk, N.; Pinks, K.; Salpadoru, T.; Cotton, K.; Michka, O.; Patrauchan, M.A.; Wozniak, K.L. Non-Antibiotic Antimony-Based Antimicrobials. *Molecules* **2022**, *27*, 7171. <https://doi.org/10.3390/molecules27217171>

Academic Editor: Carlo Santini

Received: 19 September 2022

Accepted: 14 October 2022

Published: 23 October 2022

Publisher's Note: MDPI stays neutral with regard to jurisdictional claims in published maps and institutional affiliations.



Copyright: © 2022 by the authors. Licensee MDPI, Basel, Switzerland. This article is an open access article distributed under the terms and conditions of the Creative Commons Attribution (CC BY) license (<https://creativecommons.org/licenses/by/4.0/>).

1. Introduction

Microbial infections are associated with considerable morbidity and costs. The continuous spread of antimicrobial resistance (AMR) among bacterial and fungal pathogens imperils the usefulness of antibiotics and antifungals, which previously revolutionized and enabled medical interventions. The increasing AMR is manifesting as multidrug resistance (MDR), leading to a global crisis that, if not addressed, will soon have a huge adversarial impact on human race. The main causes of the rapid increase in AMR include an overuse of antimicrobials, inappropriate prescribing, and the inability of patients to follow the prescribed drug regimen. Extensive use of antibiotics in agricultural settings and the wide availability of some antibiotics are also important factors. This situation led to the appearance of antibiotic resistant bacterial pathogens, exemplified by methicillin-resistant *Staphylococcus aureus* (MRSA), and vancomycin-resistant enterococci (VRE), which are becoming increasingly difficult to treat with the current range of available antibiotics. Fungal pathogens *Cryptococcus neoformans* and *Candida albicans* are also becoming increasingly resistant to antifungal drugs, and different *Candida* species with natural drug resistance,

such as *Candida auris*, are evolving in hospital settings and becoming major pathogens. The MDR phenomenon is one of the greatest global public health challenges that humanity is currently facing. According to the Centers for Disease Control and Prevention (CDC) report on antimicrobial resistance conducted in 2019, annually, there are more than 2.8 million antibiotic-resistant bacterial infections, from which more than 35,000 people die in the US. Although fungal drug-resistant strains are more difficult to track, current estimates indicate that fungal infections lead to more than 1.5 million deaths annually worldwide. Additionally, the economic impact due to treating these infections, as well as the loss of productivity, is astronomical—about 4.6 billion USD annually for bacterial infections and about 7.2 billion USD annually for fungal infections.

With modern medicine's reliance on antimicrobials in treating diseases such as pneumonia, tuberculosis, sexually transmitted diseases, and bloodstream infections, the problem with AMR is that, soon, no current treatments will be effective. Therefore, the development of new antimicrobial agents is imperative. The critically important progress in this field requires the development of new chemical compounds that would inhibit bacterial and/or fungal growth while not being toxic to human tissues. Pure organic compounds, which classic antibiotics are, cannot meet these criteria, as they can be metabolized by microorganisms or lead to the development of resistance. In contrast, inorganic salts and Werner-type complexes may offer an alternative with the required properties.

The successful application of metal complexes and organometallic compounds in the treatment of numerous human diseases is a vigorously expanding area in both biomedical and bioinorganic chemistry research. Remarkably, the group XV elements in the periodic table—pnictogens—contain all biologically active elements. Nitrogen (N) and phosphorus (P) are crucial for life on the planet, while arsenic (As), antimony (Sb), and bismuth (Bi) possess very useful properties for various biomedical applications. Paul Ehrlich, widely known as the father of antimicrobial chemotherapy and bioinorganic chemistry, found the "magic bullet" (compound 606) capable of treating the highly infectious bacterial pathogen *Treponema pallidum* without hurting the host. This compound is a heterocyclic arsenic-based small molecule ($C_{12}H_{13}As_2C_1N_2O_2$) that was used to successfully treat syphilis and was marketed as Salvarsan ("lifesaving") [1]. Despite the well-known toxicity of arsenic, this drug saved >560,000 lives within 50 years [2]. Bismuth, contrary to arsenic, is not toxic and is widely used as subsalicylate ($C_7H_5BiO_4$) in the well-known drug Pepto-Bismol [3]. In turn, antimony has been used since early Egyptian's civilization [4]. For example, $NaSbO_3$ was commonly used as an emetic compound until the late 1700s [5]. The other successful application of Sb is the treatment of leishmaniasis, caused by a protozoan parasite *Leishmania* transmitted through the bite of infected sandflies in South and Central America, Bangladesh, southern Europe, and North Africa. The active compounds against the disease were found to be several Sb(V) carbohydrates, such as sodium antimony gluconate (Pentostam) and meglumine antimonate (Glucantime). These have been in use for more than six decades to treat leishmaniasis [6]. In all these active Werner-type complexes, there is an $[SbO_6]$ environment. Furthermore, several organoantimony compounds have been studied and shown to possess antimicrobial, antifungal, and antitumor activities [7–13]. In such case, the chemical (toward hydrolysis) and thermodynamic stability of the Sb–C bond seems to be a favorable factor for biological activity and lessening of side-effects contrary to the abovementioned Sb-carbohydrates.

Cyanoximes (Figure 1) represent a new subclass of small organic molecules—oximes, the chemistry and applications of which have been intensely developed during the last two decades [14–17]. Cyanoximes and their metal salts and Werner-type complexes demonstrate a large spectrum of biological activity: pesticide antidotes [18,19], antimicrobial [20,21], and growth regulation in plants [22,23]. Recently, it was discovered that Sb(V) cyanoximates are thermally and chemically stable in both solid state and solutions [24].

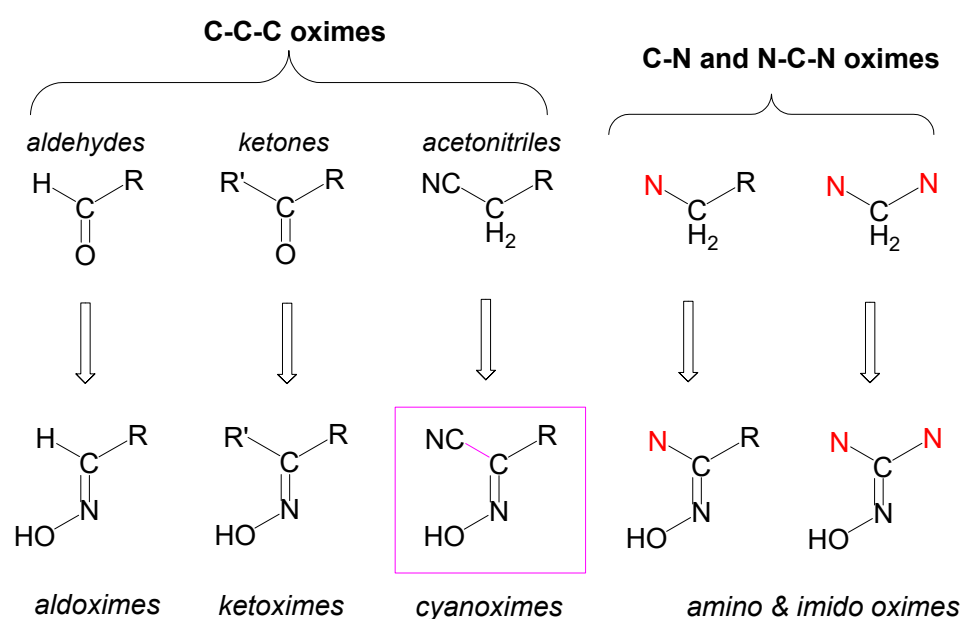


Figure 1. Types of oximes and their precursors.

In addition, no intrinsic *in vitro* cytotoxicity was detected for free cyanoximes, organic ligands used to synthesize organoantimony(V) compounds [25–27]. Thus, it is an attractive idea to explore the potential synergistic effect of both by combining the known biological activity of cyanoximes with the established medical use of antimony(V) compounds. The aim of this study was to develop new, non-antibiotic antimicrobial compounds that efficiently inhibit pathogenic bacteria and fungi. On the basis of our previous biomedical investigations of 48 currently known cyanoximes [14], we selected eight cyanoximes shown in Figure 2 for the preparation, characterization, and subsequent antimicrobial studies of new tetraphenyl-antimony(V) cyanoximates. The choice of these acido-ligands was founded primarily on their water solubility and biological activity. Furthermore, using the series of novel organoantimony compounds, we initiated the investigation of the structure (biological)–activity relationship (SAR), focusing on the effect of O vs. S atoms in the structure, bulkiness of the cyanoxime, or effect (if any) of cyclic groups vs. alkyl groups present in the ligand. In this paper, we present the preparation, characterization, and biological activity studies of the first generation (designated as G1) of new tetraphenyl-antimony(V) cyanoximates SbPh_4L .

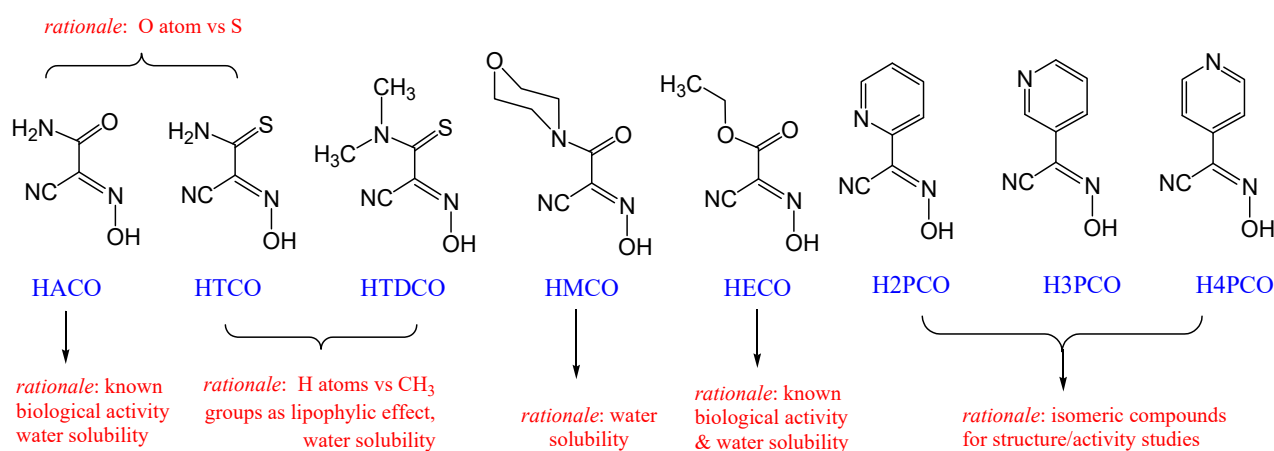
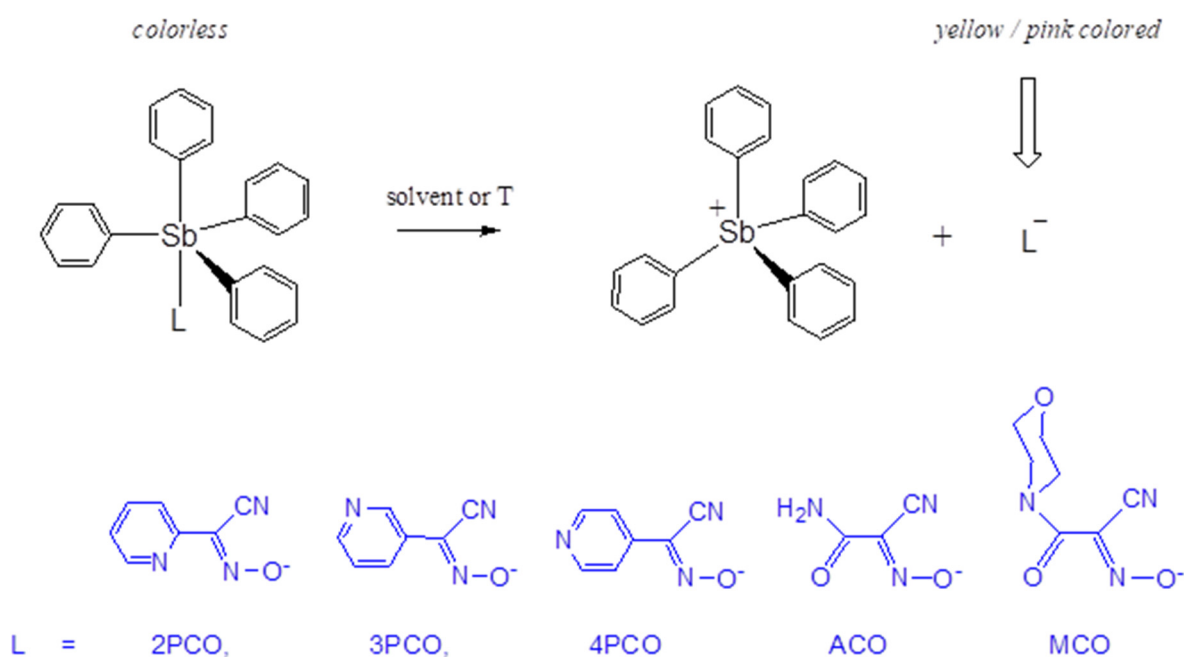


Figure 2. Chemical structures of cyanoximes used in this work, together with their commonly adopted abbreviations, and rationalized choice for these specific compounds.

2. Results and Discussion

Chemical Aspect

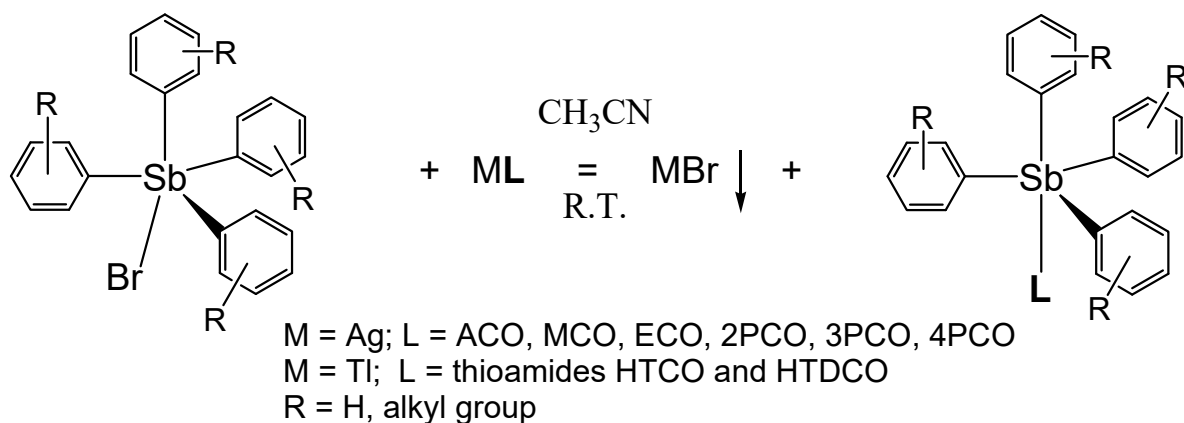
The starting compound SbPh_4Br is only one commercially available source of pentavalent antimony with four organic groups attached. In this project, we used this compound for the preparation of the first series (G1) of organoantimony(V) cyanoximates for systematic antimicrobial studies. In the past, we found that the metathesis reaction of beforehand prepared Ag(I) of cyanoxime salts with other organoelemental compounds of Te(IV) [28], Sn(IV) [26,29], and Sb(V) [24] was a very successful approach for the high-yield synthesis of desired elementorganic cyanoximates (Scheme 1). Quantitative preparation of silver(I) cyanoximates has been developed in our group [30–33] (Scheme 2A). In this work, we expanded the utility of the metathesis reaction in dry organic solvents with Tl(I) cyanoximates (Scheme 1) and applied it to synthesize a series of Sb(V) compounds. These compounds were prepared practically quantitatively in warm aqueous solutions using Tl_2CO_3 as the source for the heavy-metal cation [16,34,35] (Scheme 2B). Thus, we showed that the use of Tl(I) salts is equally useful and convenient when desired Ag-salts for other cyanoximates are either not obtainable or difficult to handle because of their high light sensitivity and thermal instability. Moreover, thallium(I) is not an oxidizer contrary to silver(I) salts, while Tl(I) compounds are not light sensitive and thermally stable [36], yet quantitatively form halogenides insoluble in water and common organic solvents. These factors make work with Tl(I) derivatives attractive; however, all necessary precautions should be taken due to their toxicity as explained in the *Safety Note* in Section 3.



Scheme 1. Representation of the color gain of solutions of organoantimony(V) cyanoximates in the case of the compounds covalent integrity breaking down.

Crystal structures were determined for all eight obtained organoantimony(V) compounds, but only six are presented in this work (Figure 3). Two structures with thioamide-cyanoximes TCO^- and TDCO^- showed interesting peculiarities (polymorphism) and will be published in a more specialized in crystallography journal. However, both structures are only briefly presented in the Supporting Information section SI S22. In light of the description of this new family of Sb-based organometallic compounds, it is necessary to mention that previous biomedical research with this element focused only on compounds with traditional donor–acceptor or covalent Sb–O bonds. Thus, Sb–C bonding in organoantimony compounds is different from classic complexes and is significantly stronger (Figure 4). Organometallic compounds have great advantages in such a situation.

This makes these compounds stable with respect to hydrolysis reactions in aqueous media. In all eight obtained and studied tetraphenyl-antimony(V) cyanoximates, the anion is bound to the central atom in monodentate fashion via the oxygen atom of the *oxime* group (Figure 3) as can be judged from longer N–O bonds in comparison with the C–N bond in the cyanoxime molecule.



Scheme 2. Synthetic route to organoantimony(V) cyanoximates.

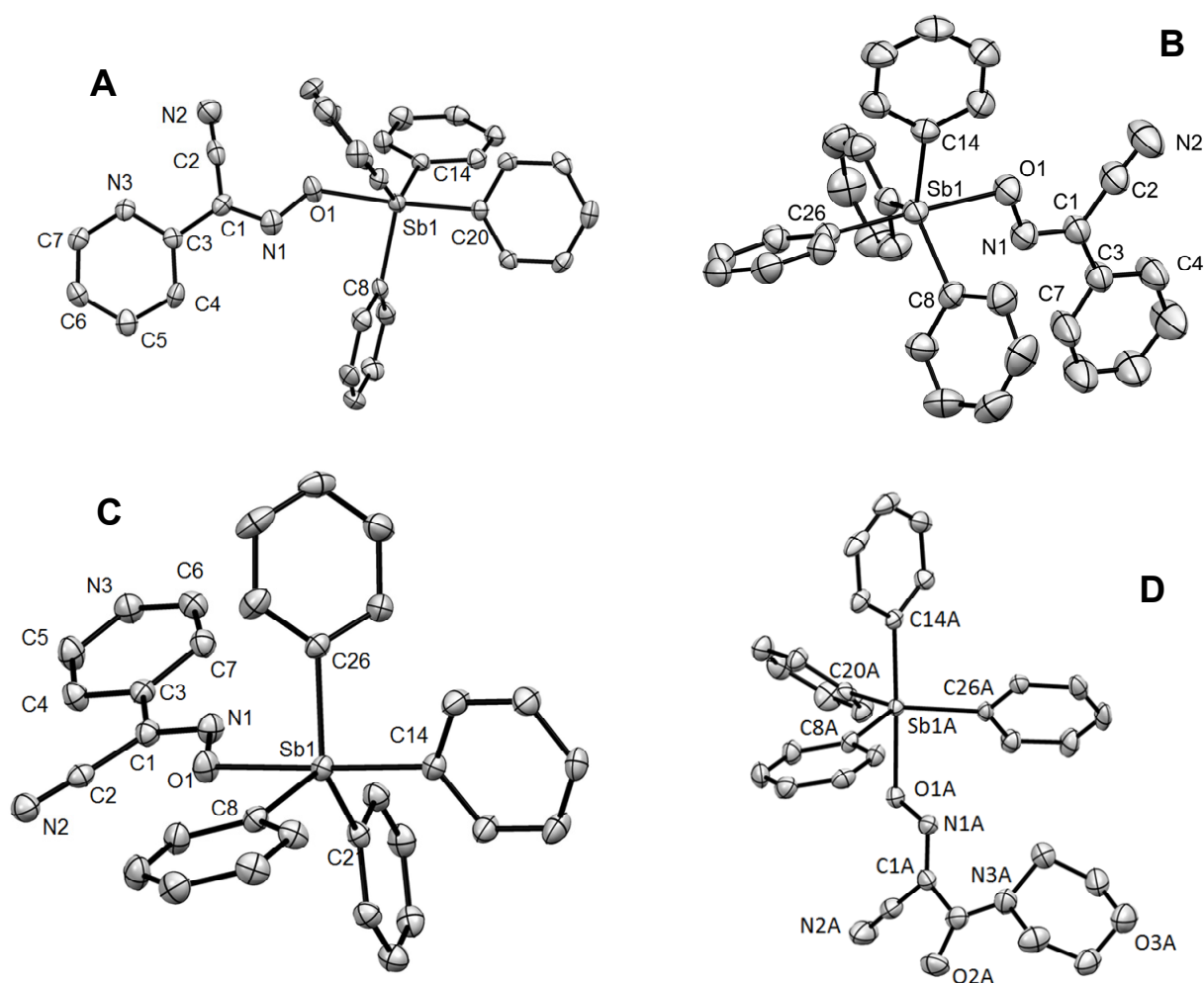


Figure 3. Cont.

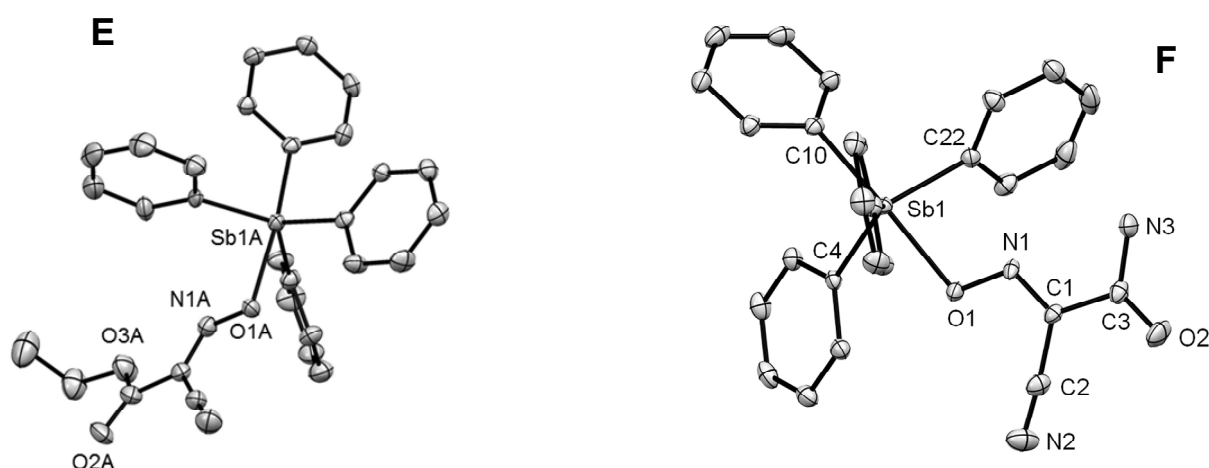


Figure 3. The ASU in the structures of $\text{SbPh}_4(2\text{PCO})$ (A), $\text{SbPh}_4(3\text{PCO})$ (B), $\text{SbPh}_4(4\text{PCO})$ (C), and $\text{SbPh}_4(\text{MCO})$ (D); only one of two independent molecules is displayed. $\text{SbPh}_4(\text{ECO})$ (E) (only one of two independent molecules present) and $\text{SbPh}_4(\text{ACO})$ (F), showing numbering of principal atoms only. Details of the geometry of crystal structures are presented in SI section. H-atoms are omitted for clarity.

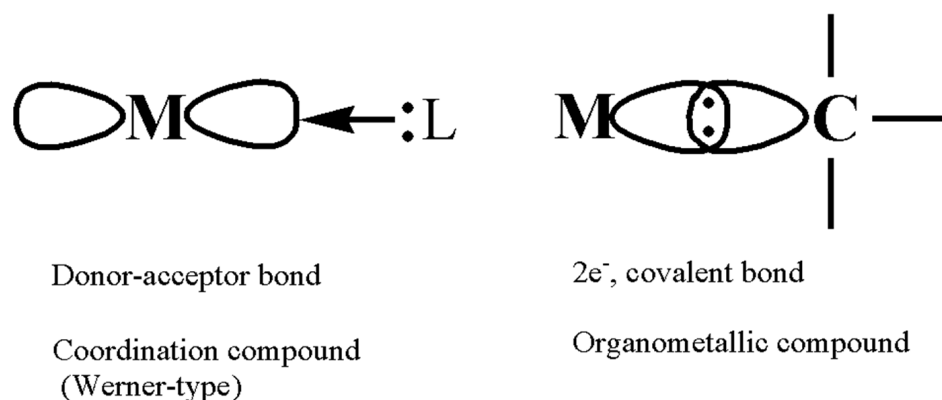


Figure 4. Simplified types of bonding found in coordination and organometallic compounds.

The best description of the geometry of molecular geometries of all studied SbPh_4L (L = cyanoxime from Figure 2) is distorted trigonal bipyramid (Figure 3). The central Sb-atom is outside of the equatorial plane in all structures and shifted toward the axial phenyl group. Thus, there is a certain “off-plane” distance in the $[\text{SbC}_3]$ equatorial environment. The geometries and the environment of Sb-centers in all compounds reported here are presented in detail pages of Supporting Information section SI S14–S22.

Further analysis of the crystal structures revealed a correlation between structures and pK values of cyanoximes coordinated to the metalloid atom (Figures 5 and 6). Thus, an inverse from the expected trend was observed; a more acidic cyanoxime bound to the metalloid led to a longer Sb–O bond length (Figure 5). Similarly, an inverse from expected trend was observed during analysis of the acidity of the cyanoxime and deviation from planarity of the $[\text{SbC}_3]$ base. Here, a more acidic cyanoxime bound to the metalloid led to the Sb-atom being more pushed inside the trigonal pyramidal cage toward the axial phenyl group (Figure 6).

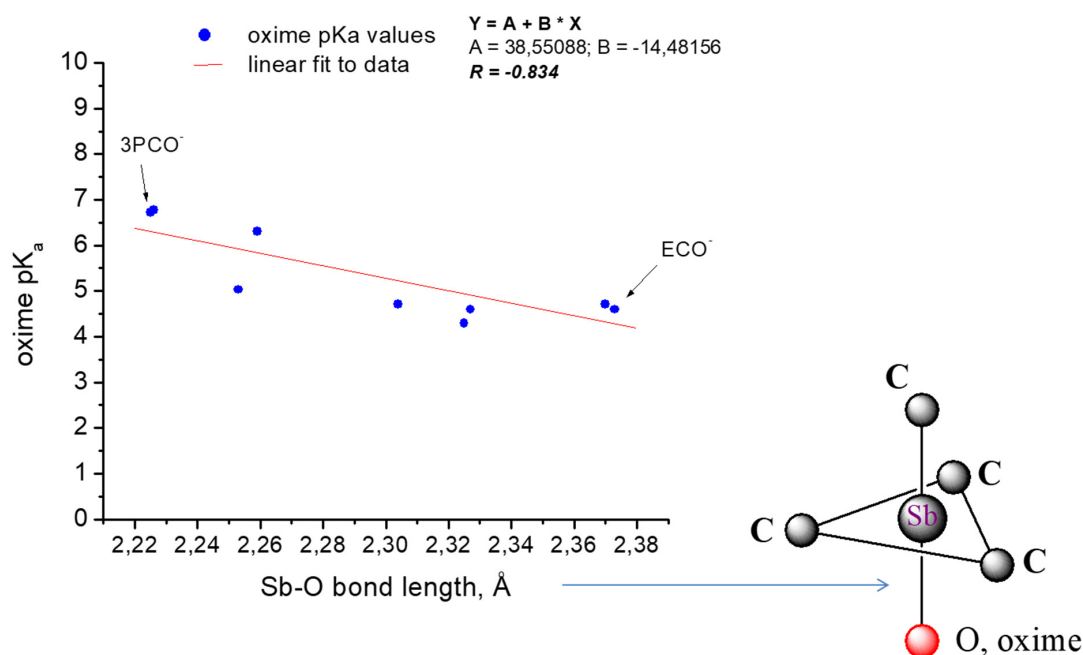


Figure 5. Observed trend in geometry of the antimony(V) environment and acidity of coordinated bond to cyanoxime moiety: Sb–O bonds vs. acidity of the cyanoxime.

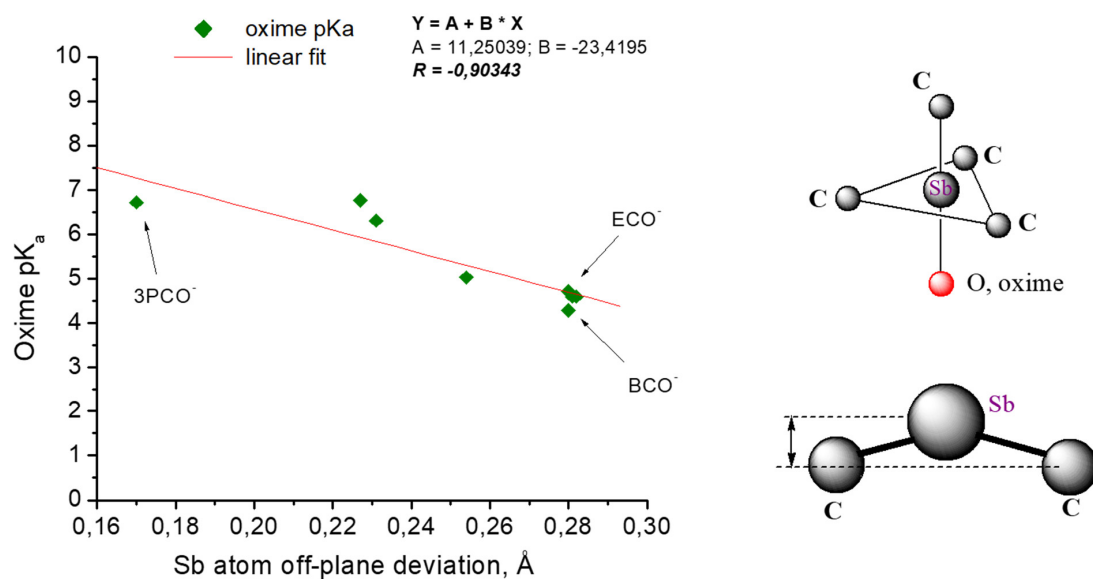


Figure 6. Observed correlation in geometry of the antimony(V) environment such as out-of-plane distance and acidity of coordinated to it cyanoxime moiety.

To continue characterization of the new family of new compounds, we investigated the thermal stability of synthesized SbPh_4L both in solutions and in a solid state. This is important for two reasons: (1) application of these new antimicrobial compounds may include using them as additives in surface coating and making wound dressing materials suitable for thermal sterilization; (2) the stability and chemical integrity in solutions at variable temperatures are important for their shelf lifetime and usability. We determined that compounds are soluble in a variety of solvents and form molecular solutions with no electrical conductivity.

The results evidenced a satisfactory stability of pure solid samples of all eight SbPh_4L at $\sim 150^\circ\text{C}$, which makes them suitable for applications that require heating or heat sterilization. The TG/DSC traces for one compound showing phase transition (melting) are

presented in SI S23, accompanied by the summary of thermal stability of studied compounds. Similarly, synthesized compounds were stable in high-boiling-point solvents such as DMSO and propionitrile. More specifically, the method of variable-temperature UV/visible spectroscopy was used in this study. Thus, all obtained organoantimony(V) cyanoximates represent colorless compounds (except for $\text{SbPh}_4(\text{TCO})$ and $\text{SbPh}_4(\text{TDCO})$, which were yellow because of the color of the thio-cyanoxime ligands TCO^- and TDCO^- (SI S1)). However, cyanoxime anions ACO^- , ECO^- , and MCO^- , and isomeric pyridyl-cyanoximes 2PCO^- , 3PCO^- , and 4PCO^- in chosen solvents appeared rose-pink due to the $n \rightarrow \pi^*$ transition in the visible region of the spectrum [37], which is sensitive to the nature of the solvent. Therefore, the appearance of color in colorless solutions of our SbPh_4L would be indicative of their dissociation and liberation of the colored anion in solution (Scheme 1).

Furthermore, we performed recording of the UV/visible spectra of all colorless organoantimony(V) cyanoximates in selected solvents from room temperature to 80°C in 10°C intervals. The results indicate the absence of appreciable ionization of cyanoximes in solutions even at elevated temperatures (Figure 7). This assures that the observed antimicrobial effects are associated with the molecular structure of the parent compound SbPh_4L (L = studied cyanoximes anion) and not to separate SbPh_4^+ and L^- ions.

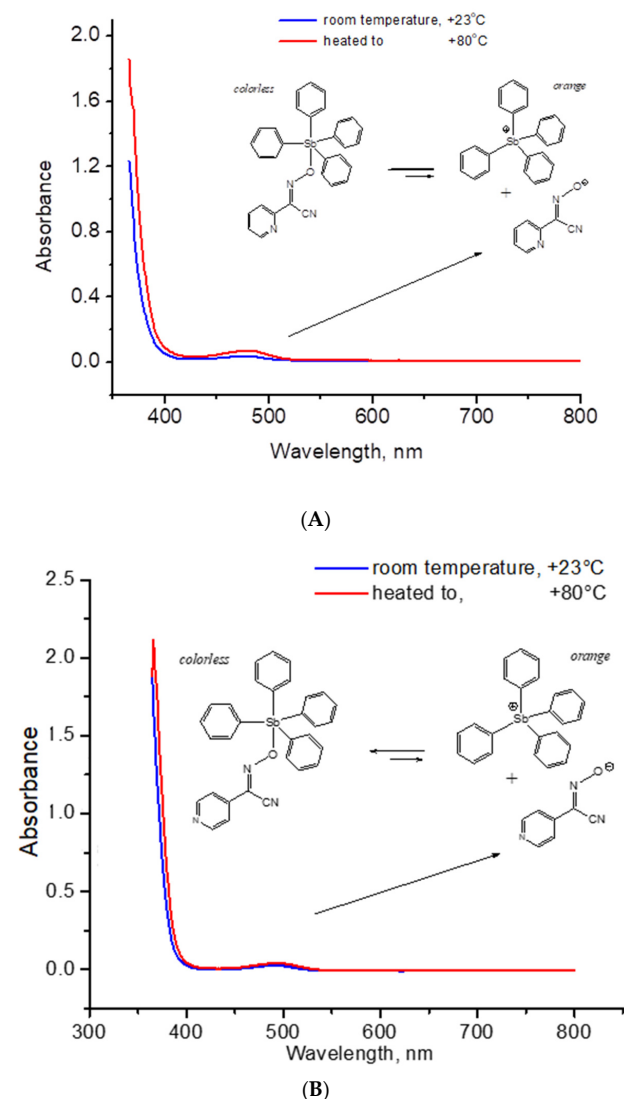


Figure 7. (A) An overlay of fragments of the UV/visible spectra of $\text{SbPh}_4(2\text{PCO})$ in DMSO at two terminal temperatures; (B) an overlay of fragments of the UV/visible spectra of $\text{SbPh}_4(4\text{PCO})$ in propionitrile at the same two terminal temperatures.

All synthesized tetraphenyl-antimony(V) compounds were characterized by $^{13}\text{C}\{^1\text{H}\}$ -NMR spectroscopy. First of all, we should note that, despite considerable concentrations of complexes used during the NMR analysis, we had difficulties in obtaining high-resolution and good-quality spectra even after ~12 h of accumulation. We attribute this unexpected difficulty to the effect of quadrupole nuclei of ^{121}Sb (57.3% abundance; $I = +5/2$) and ^{123}Sb (42.7 % abundance; $I = +7/2$) isotopes that most likely adversely affected the relaxation times of carbon nuclei.

Since it was such an unusual finding, we validated the observations by independently recording $^{13}\text{C}\{^1\text{H}\}$ -NMR spectra at different locations (Courtesy of Dr. Sergiy Tyukhtenko, Center for Drug Discovery, Northeastern University), but unfortunately with the same result. In comparison to a typical ^{13}C -NMR spectrum displayed in SI S9–S11, we observed an interesting correlation between position of the *ipso*-carbon atom of the phenyl-groups in SbPh_4L (L = cyanoximes from Figure 2) and pK_a values of the coordinated to Sb-center cyanoximes as shown in SI S24. There were two clearly different trends: one for isomeric heterocyclic cyanoximes and another for other carboxylates and amides. No immediate rationale for the observed behavior is available at the moment.

Biological Aspect

Antibacterial potential of new tetraphenyl-antimony(V) cyanoximates. It should be especially mentioned that the new cyanoximates synthesized and characterized in this work represent organometallic compounds with relatively strong Sb–C covalent bonds. They do not undergo hydrolysis in the cell contrary to previously known above-cited Werner-type complexes containing labile Sb–O bonds. The presence of lipophilic organometallic fragment provides different and favorable kinetics for the intake of tetraphenyl-antimony(V) cyanoximates into cells, which helps in the delivery of biologically active cyanoxime. Furthermore, these types of small-molecule compounds were never previously exposed to pathogenic microorganisms, which is an advantage of using these new antimicrobial compounds until resistance to them is potentially developed decades later.

To determine the antibacterial potential of the novel antimony compounds, we selected three human pathogens: Gram-negative *E. coli* and *P. aeruginosa*, and Gram-positive *S. aureus*. The Shiga toxin-producing *E. coli* strain S17 (O113:H4) was isolated from a chick liver with septicemia [38], the lab-adapted *P. aeruginosa* strain PAO1 was originally isolated from a burn-wound infection [39], and the methicillin-resistant *S. aureus* strain NRS70 was isolated from a respiratory infection [40]. These pathogens represent different infection profiles. Both *P. aeruginosa* and *S. aureus* are becoming increasingly resistant to currently available antibiotics [41,42] and were recognized by the CDC as critically important for discovering novel therapeutics. All three strains were subjected to disc-diffusion assay (Table 1, SI S25).

Table 1. Antibacterial effect of new tetraphenyl-antimony(V) cyanoximates determined by disc-diffusion assay. The zones of clearance (mm) surrounding the discs are reported as the averages from three samples \pm SEM. ND, no clearance zone detected.

Compound/Clearance Zone, mm	<i>E. coli</i>	<i>P. aeruginosa</i>	<i>S. aureus</i>
Sb Compounds			
SbPh ₄ (ACO)	2.5 \pm 0.2	5.6 \pm 0.7	4.7 \pm 0.7
SbPh ₄ (ECO)	4.7 \pm 0.2	2.2 \pm 0.3	9.4 \pm 0.1
SbPh ₄ (MCO)	ND	5.7 \pm 0.2	6.1 \pm 0.1
SbPh ₄ (TDCO)	ND	ND	2.0 \pm 0.5
SbPh ₄ (TCO)	ND	ND	ND
Controls			
H(ACO)	ND	ND	ND
H(ECO)	ND	ND	ND
H(MCO)	ND	ND	ND

Among the antimicrobial compounds tested, SbPh₄(ACO) and SbPh₄(ECO) showed activity against all three bacterial pathogens. SbPh₄(MCO) was effective against *P. aeruginosa*

and *S. aureus*, and SbPh₄(TDCO) showed activity only against *S. aureus* (Table 1, SI S26). Three control compounds H(ACO), H(ECO), and H(MCO) were tested and showed no antimicrobial effect. The results showed that the cyanoximates alone have no antimicrobial impact, and the incorporation of the SbPh₄ fragment into selected backbones enables the antimicrobial potential. Comparison of two (twofold and fourfold) dilutions for each compound reflected concentration-dependent growth inhibition for most of the compounds, except for SbPh₄(ACO) (*E. coli*), SbPh₄(ECO) (*P. aeruginosa*), and SbPh₄(TDCO) (*S. aureus*) (SI S27). This may reflect a time-dependent antimicrobial effect [43]. According to the inhibition profile, SbPh₄(ACO), SbPh₄(ECO), and SbPh₄(MCO) do not discriminate between Gram-negative and Gram-positive bacteria, suggesting that their broad impact on bacterial cells is independent of the presence or absence of the outer membrane of Gram-negative cells and peptidoglycan of Gram-positive cells. The SbPh₄(TDCO) activity only against Gram-positive *S. aureus* suggests that the outer membrane of Gram-negative *E. coli* and *P. aeruginosa* presents a sufficient protective barrier for this compound. These results confirm that the new antimony compounds have strong potential as both broad- and narrow-spectrum antimicrobials and provide insights for further synthetic modifications of the compounds to increase their activities.

Antifungal potential of new tetraphenyl-antimony(V) cyanoximates. To determine the antifungal potential of the novel antimony compounds against fungal pathogens, we selected two human fungal pathogens—*Cryptococcus neoformans* and *Candida albicans*. Both *C. neoformans* and *C. albicans* are becoming increasingly resistant to currently available antifungals [13,44–46], and resistance is being tracked through the CDC’s Emerging Infections Program (EIP). Both strains were subjected to a disc-diffusion assay (Table 2). Among the compounds tested, SbPh₄(MCO) was the only compound to inhibit the growth of both fungal pathogens *C. neoformans* and *C. albicans*. The remaining compounds inhibited the growth of *C. neoformans* but not *C. albicans* (Table 2, SI S28). These results confirm that the new antimony compounds have a strong potential, especially against the fungal pathogen *C. neoformans*, but they may need further synthetic modifications to be active against *C. albicans*.

Table 2. Antifungal effect of new tetraphenyl-antimony(V) cyanoximates determined using a disc-diffusion assay. The zones of clearance (mm) surrounding the discs are reported as diameters averaged from three samples ± SEM. ND, no clearance zone detected.

Compound/Clearance Zone, mm	<i>C. neoformans</i>	<i>C. albicans</i>
Sb Compounds		
SbPh ₄ (ACO)	6.7 ± 1.3	ND
SbPh ₄ (ECO)	9.7 ± 4.4	ND
SbPh ₄ (MCO)	5.0 ± 1.3	2.9 ± 1.2
SbPh ₄ (TDCO)	2.0 ± 1.0	ND
SbPh ₄ (TCO)	2.7 ± 1.3	ND
Controls		
H(ACO)	ND	ND
H(ECO)	ND	ND
H(MCO)	ND	ND

We observed a pronounced synergistic effect of the presence of organoantimony(V) and cyanoxime moieties in these molecular compounds. The results of the conducted interdisciplinary research warranted filing full patent application No. 63/152,490 “Organoantimony(V) cyanoximate compounds and methods of production and use thereof”, filed on 23 February 2022. On 6 September 2022, the US Patent and Trademark Office informed us that the above-referenced PCT application was published as International Publication No. WO2022/182719 A1, with an International Publication Date of 1 September 2022.

3. Materials and Methods

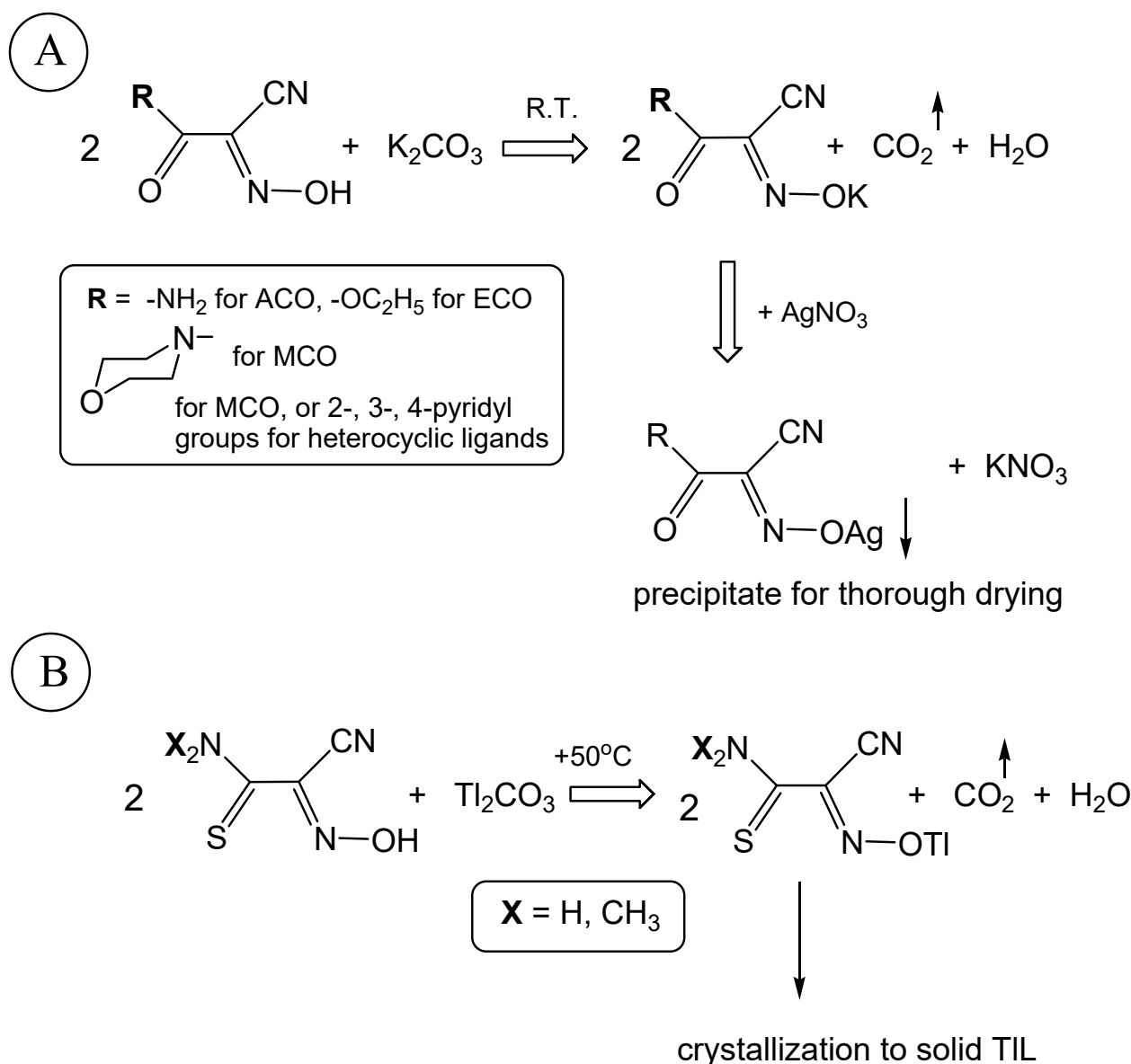
Chemistry.

General Considerations. Cyanoximes selected for current studies were obtained using published procedures from starting substituted acetonitriles [14], and their purity was verified using TLC, NMR spectroscopy, and elemental analyses of C, H, N content using combustion method (Atlantic Microlab, Norcross, GA). Starting compounds with sulfur-containing cyanoximes Tl(TCO) and Tl(TDCO) were also prepared as we described earlier [34,47]. The source of organoantimony, ~95% purity, was Sb(C₆H₅)₄Br purchased from Aldrich. All other chemicals and organic solvents—*i*-PrOH, CH₃CN, ether, NaNO₂, H₂SO₄, and HCl from Fisher Scientific and sodium metal from Fluka—were of sufficient quality and used without additional purification. Melting points and thermal decomposition profiles were obtained using thermal analysis method presented below. Electrical conductivity of 0.001 M solutions of SbPh₄L (L = cyanoximes shown in Figure 2) was measured in CH₃CN and DMSO at 296 K with aid of the YSI 3100 conductivity meter with Pt-electrode using N(CH₃)₄Br and P(C₆H₅)₄Cl salts as calibrants.

Chemical Synthesis. Preparation of cyanoximes shown in Figure 2 was conducted according to the published procedures for HACO [30], HACO [21], HTDCO [47], HECO [48], HMCO [31], and isomeric pyridyl-cyanoximates [35]. The source of antimony was bromide of tetraphenyl-antimony(V). We determined that the best synthetic route to organometallic cyanoximates is a metathesis reaction of Ph₄Br with silver or thallium cyanoximates, as shown in Scheme 2. The latter salt was used for the S-containing cyanoximes HTCO and HTDCO for which corresponding silver(I) salts do not exist due to fast decomposition with the formation of Ag₂S, while Tl(TCO) and Tl(TDCO) [34,47] can be easily obtained and are thermally and light stable. The typical preparation is given only for two tetraphenyl-antimony(V) cyanoximates.

Silver(I) salts of ligands listed in Scheme 2 are light-stable and were obtained in aqueous solutions in two steps as shown in Scheme 3A using AgNO₃ [32,49], while two thallium(I) salts were prepared from Tl₂CO₃ (Scheme 3B). The actual appearance of dark-yellow and orange TIL (L = TCO, TDCO) can be seen in Supporting Information, S1.

SbPh₄(MCO). The preparation of SbPh₄(MCO) was conducted by dissolving 0.201 g (0.394 mM) of SbPh₄Br in 10 mL of dry acetonitrile in a 25 mL Erlenmeyer flask to which 0.120 g (0.413 mM, being in slight excess because of heterogeneous reaction) of finely ground, solid Ag(MCO) [31] was added in small portions under stirring at room temperature. This reaction requires red-light (or dark) conditions to prevent photodecomposition of the light-sensitive byproduct AgBr. Use of an ultrasound bath is necessary to assure proper reagent mixing in this heterogeneous reaction. Following sonication, removal of the white AgBr precipitate was found to be the most convenient by centrifugation using nylon 0.45 micron membrane inserts into 5 mL Eppendorf tubes (SI S2). Thus, the cloudy reaction mixture of the desired organoantimony(V) cyanoximate in CH₃CN solution and fine powder of AgBr was transferred into nylon Eppendorf tubes and centrifuged in a Thermo Scientific Sorvall Legends Micro 17 at 10,000 rpm for 3 min. The colorless and transparent solution containing SbPh₄(MCO) was carefully pipetted from the tube into 25 mL beaker placed into a charged with a paraffin (for absorption of CH₃CN) vacuum desiccator for further crystallization. After 1 week, colorless block-type crystals of the complex suitable for the X-ray analysis were harvested from the beaker.



Scheme 3. Preparation of precursors—silver and thallium salts—for synthesis of SbPh₄L.

SbPh₄(TCO). Synthesis of this compound involved 0.250 g (0.490 mM) of SbPh₄Br and 0.170 g (0.511 mM, slight excess due to heterogeneous reaction condition) of a yellow powder of Tl(TCO) mixed together with 10 mL of dry CH₃CN in a 25 mL beaker at room temperature. The preparation of Tl(TCO) is described in Supporting Information section SI S3, while Tl(TDCO) synthesis was carried out according to a published procedure [30] with results of the elemental analysis displayed in SI S1. Since Tl(I) salts are non-oxidizers and not light-sensitive, the reaction was carried out conveniently on a bench top. Thorough mixing of reagents in this heterogeneous reaction was performed in an ultrasound bath within 10 min. The content of the beaker as a fine yellow suspension was placed in Eppendorf tubes and centrifuged within 3 min at 10,000 rpm, leading to clean separation of the white TlBr and transparent yellow solution of target compound. Careful pipetting of this solution into another beaker followed by its concentration in a vacuum desiccator, charged with paraffin to absorb CH₃CN, afforded light-yellow transparent plates (SI S4).

Other compounds were prepared in a similar fashion. Information regarding the synthesized compounds' color, yield, and results of elemental analyses presented in Table 3.

Table 3. Yield, color, and composition of the obtained tetraphenyl-antimony(V) cyanoximates and two of their precursors: Tl(I) salts.

Formula, Property			Elemental Analyses Data, %: Calculated (Found)			
Compound	Color	Yield, %	C	H	N	S
SbPh ₄ (ACO)	Colorless	79	59.81 (58.39)	4.09 (4.16)	7.75 (7.29)	-
SbPh ₄ (ECO)	Colorless	91	60.86 (60.59)	4.58 (4.44)	4.89 (4.94)	-
SbPh ₄ (TCO)	Yellow	51	58.04 (57.93)	3.97 (3.84)	7.53 (7.42)	5.74 (5.59)
SbPh ₄ (TDCO)	Golden-orange	56	59.40 (58.84)	4.47 (4.37)	7.17 (6.20)	5.47 (5.18)
SbPh ₄ (MCO)	Colorless	90	60.81 (59.48)	4.61 (4.52)	8.86 (6.47)	-
SbPh ₄ (2PCO)·H ₂ O	Colorless	45	64.61 (64.34)	4.20 (4.07)	7.29 (7.19)	-
SbPh ₄ (3PCO)	Colorless	84	64.61 (62.17)	4.20 (3.99)	7.29 (6.51)	-
SbPh ₄ (4PCO)	Colorless	46	64.61 (63.93)	4.20 (3.93)	7.29 (7.31)	-
Tl(TCO)	Yellow	93	10.84 (10.77)	0.61 (0.54)	12.64 (12.71)	9.64 (9.52)
Tl(TDCO)	Orange-red	82	16.66 (16.61)	1.68 (1.55)	11.65 (11.53)	8.89 (8.77)

Safety Note: Although we did not encounter any problems during many years of laboratory work and handling, special care should be taken during work with thallium compounds because of their high toxicity [50–52]. Both Tl(I) carbonate and cyanoximates are water-soluble compounds, which emphasizes the absolute necessity of always wearing protective gloves when working with these compounds. However, no respiratory tract covers are required since Tl(I) compounds are ionic and not volatile.

Spectroscopic Studies.

Vibrational spectra. The IR spectra of all the prepared compounds reported herein were recorded at ambient laboratory temperature using small quantities (5–10 mg) of solid samples of studies compounds with the help of a Bruker ATR FT spectrophotometer. The resolution was set to 4 cm⁻¹ with 64 scans in the range of 400–4000 cm⁻¹. An atmospheric compensation and baseline correction were applied for data treatment. Raman spectra were recorded on the Bruker R70 FT-IR/Raman complex at room temperature. The power of the laser and the number of repetitions were varied depending on the sample in the ranges of 100–250 mW and 64–1024 scans, respectively. The combined results of vibrational spectroscopy as assigned peaks of the most important vibrations in spectra are presented in Table SI S5.

UV/visible spectra. The electronic spectra of the compounds were recorded in solutions using the HP 8354 diode array UV/visible spectrophotometer operating in the range of 200–1100 nm, typically at room temperature. In cases where variable-temperature spectra were needed, a high-precision Peltier Quantum Northwest thermocontroller was used with 1 cm quartz cuvettes.

NMR spectra. The ¹H- and ¹³C{¹H}-NMR spectra were obtained on a Varian Inova-400 MHz spectrometer at room temperature in CD₂Cl₂ containing TMS as an internal reference. Data are tabulated in SI S6–S8, whilst several selected spectra are displayed in SI S9–S11.

X-ray crystallography.

Crystal structures were determined for all the eight organoantimony(V) compounds. Suitable single crystals of organoantimony(V) cyanoximates were grown at 4 °C exclusively using the vapor diffusion method. Briefly, acetonitrile solutions of compounds were placed into the inner tube, and vapors of anhydrous ether were used as the crystallizing agent from the outer tube with a screw cap. Normally within 2–3 weeks after setting up, transparent well-shaped crystals suitable for crystallographic studies appeared on the walls in the inner tube. All crystals suitable for studies were placed on plastic MiTeGen holders attached to the copper pin on the goniometer head of the Bruker APEX-2 diffractometer, equipped with a SMART CCD area detector. The intensity data were collected at low tem-

perature. Data collection was performed in ω scan mode using the Mo tube (K_{α} radiation; $\lambda = 0.71073 \text{ \AA}$) with a highly oriented graphite monochromator. Intensities were integrated from four series of 364 exposures, each covering 0.5° steps in ω at 20–60 s of exposure time depending on the crystal diffracting power, with the total dataset being a sphere. The space group determination was conducted with the aid of the XPREP software. The absorption correction was performed in a few cases by a crystal face indexing procedure with the help of a video microscope (SI S12,S13), followed by numerical input into the SADABS program. Ultimately, in the case of a small crystal specimen and their irregular shape, we used the multi-scan method. Both cited programs are included in the Bruker AXS software package [53]. All structures were solved using direct methods and refined by least squares on weighted F^2 values for all reflections using the SHELXTL program. In several structures, due to the high crystal quality, it was possible to identify all H-atoms on the electron density map. However, in some structures, H-atoms were placed in calculated positions in accordance with the hybridization state of a hosting carbon atom and were refined isotropically. No apparent problems or complications were encountered during the structure solutions and refinement as evident from very positive PLATON checkCIF reports. The crystal data for six structures of Sb-cyanoximates are presented in Table 4, while their ASUs are shown in Figure 3. Values of selected bond lengths and valence angles are presented in the respective figures in SI S14–S22. All drawings of the crystal structures were completed using the ORTEP 3v2 [54] and freely available CCDC Mercury software packages. All determined crystal structures were deposited at CCDC (England) under the following numbers: SbPh₄(MCO)—2012156 (as refcode SURYIQ); SbPh₄(ECO)—2012153 (as SURXUB), SbPh₄(4PCO)—2011863 (as SUPPAX), SbPh₄(3PCO)—2011860 (as SUPNID), SbPh₄(2PCO)—2011861 (as SUPNOJ), and SbPh₄(ACO) (as ZASVUK02). The PLATON checkCIF reports are presented at the end of the Supporting Information (SI S29).

Table 4. Crystal data for tetraphenyl-antimony(V) cyanoximates.

Data/Parameter	SbPh ₄ (ACO)	SbPh ₄ (ECO)
Chemical formula	C ₂₇ H ₂₂ N ₃ O ₂ Sb	C ₂₉ H ₂₅ N ₂ O ₃ Sb
Formula weight, g/mol	542.22	571.26
Temperature, K	100(2)	120(2)
Wavelength, Å	0.71073 Å (Mo)	0.71073 Å (Mo)
Crystal habit	Clear colorless block	Clear colorless block
Crystal system	Monoclinic	Monoclinic
Space group	P2 ₁ /c	Pn
Unit cell dimensions, Å,	a = 14.8336(8) $\alpha = 90^{\circ}$ b = 9.9060(6) $\beta = 112.7130(10)^{\circ}$ c = 17.3977(10) $\gamma = 90^{\circ}$	a = 9.7871(6) $\alpha = 90^{\circ}$ b = 14.9208(9) $\beta = 94.6130(10)^{\circ}$ c = 17.6984(11) $\gamma = 90^{\circ}$
Volume, Å ³	2358.2(2)	2576.1(3)
Z	4	4
Density (calculated), g/cm ³	1.527	1.473
Absorption coefficient μ , mm ⁻¹	1.199	1.103
F(000)	1088	1152
Θ range for data	1.49° to 33.02°	1.37° to 33.08°
Total reflections collected	38365	9092
Independent reflections	8465 [R(int) = 0.0278]	8454 [R(int) = 0.0261]
Goodness of fit on F^2	1.173	1.193 [absolute structure parameter 0.5(0)]
Final R indices	R1 = 0.0288, wR2 = 0.0634	R1 = 0.0351, wR2 = 0.0709

Table 4. Cont.

Data/Parameter	SbPh ₄ (ACO)	SbPh ₄ (ECO)
All data	R1 = 0.0391, wR2 = 0.0724	R1 = 0.0404, wR2 = 0.0774
Largest diff. peak and hole, eÅ ⁻³	2.183 and -0.805	2.218 and -1.311
Structure takes volume, Å ³ (%)	1507.45 (63.92)	1615.90 (62.73)
Chemical formula	C ₃₁ H ₂₈ N ₃ O ₃ Sb	C ₃₁ H ₂₄ N ₃ OSb
Formula weight, g/mol	612.31	576.28
Temperature, K	100(2)	100(2)
Wavelength, Å	0.71073 Å (Mo)	0.71073 Å (Mo)
Crystal habit	Clear colorless block	Clear colorless block
Crystal system	Monoclinic	Monoclinic
Space group	P2 ₁ /c	P2 ₁ /n
Unit cell dimensions, Å, °	a = 17.6451(4) α = 90 b = 10.8777(3) Å β = 94.8360(10)° c = 28.3876(7) Å γ = 90°	a = 12.6027(8) α = 90° b = 14.4415(10) β = 104.9644(10)° c = 14.6694(10) γ = 90°
Volume, Å ³	5429.3(2)	2579.3(3)
Z	8	4
Density (calculated), g/cm ³	1.498	1.484
Absorption coefficient μ, mm ⁻¹	1.054	1.098
F(000)	2480	1160
Θ range for data	1.16 to 26.52°	1.90 to 26.71°
Total reflections collected	75269	30635
Independent reflections	11251 [R(int) = 0.0612]	5458 [R(int) = 0.0520]
Absorption correction	multi-scan	multi-scan
Data/restraints/parameters	11,251/0/750	5458/0/421
Goodness of fit on F ²	1.114	1.039
Final R indices	R1 = 0.0447, wR2 = 0.1034	R1 = 0.0329, wR2 = 0.0740
All data	R1 = 0.0584, wR2 = 0.1109	R1 = 0.0444, wR2 = 0.0792
Largest diff. peak and hole, eÅ ⁻³	2.081 and -0.653	1.518 and -0.437
Structure takes volume, Å ³ (%)	3438.33 (63.33)	1625.16 (63.01)
Chemical formula	C ₃₁ H ₂₄ N ₃ OSb	C ₃₁ H ₂₄ N ₃ OSb
Formula weight, g/mol	576.28	576.28
Temperature, K	296(1)	100(2)
Wavelength, Å	0.71073 Å (Mo)	0.71073 Å (Mo)
Crystal habit	Transparent clear prisms	Transparent colorless prisms
Crystal system	Triclinic	Monoclinic
Space group	P-1	P2 ₁ /c
Unit cell dimensions, Å, °	a = 10.0228(4) α = 69.324(1) b = 10.4598(4) β = 72.086(1) c = 13.8258(5) γ = 83.971(1)	a = 15.3352(10) α = 90° b = 9.7848(6) β = 119.272(4)° c = 19.6576(9) γ = 90°
Volume, Å ³	1290.34(9)	2573.0(3)
Z	2	4
Density (calculated), g/cm ³	1.483	1.428

Table 4. Cont.

Data/Parameter	SbPh ₄ (ACO)	SbPh ₄ (ECO)
Absorption coefficient μ , mm ⁻¹	1.098	1.099
F(000)	579	1068
Θ range for data	1.15 to 28	1.50 to 33.08
Total reflections collected	22487	42357
Independent reflections	6218 [Rint = 0.0284]	9309 [Rint = 0.0223]
Absorption correction	multi-scan	numerical
Data/restraints/parameters	6218/0/421	9309/0/417
Goodness of fit on F^2	1.042	1.010
Final R indices	R1 = 0.0241, wR2 = 0.0543	R1 = 0.0286, wR2 = 0.0543
all data	R1 = 0.0276, wR2 = 0.0560	R1 = 0.0368, wR2 = 0.0603
Largest diff. peak and hole, eÅ ⁻³	0.53 and -0.34	1.91 and -0.72
Structure takes volume, Å ³ (%)	813.46 (63.04)	1639.12 (63.7)

Thermal Analysis. Thermal stability of the obtained metal complexes was assessed using a Q-600 TG/DSC analyzer (TA Instruments) under N₂ flow of 100 mL/min at a 10 °C/min heating rate. Heating of samples was carried out to 800 °C, at which complete decomposition of the samples was attained. The final product of decomposition is elemental antimony, which appears as a spongy mass inside the crucible.

Biological studies.

Susceptibility testing for bacteria and fungi using disc-diffusion assay. Discs to be tested were prepared by applying the synthesized compounds dissolved in acetonitrile at a concentration of 0.05 μ M onto 100% cotton paper discs of 7 mm width that were pre-dried in a desiccator over H₂SO₄. The loaded discs were then placed on a Teflon block to allow them to dry completely. Five Sb compounds, SbPh₄(ACO), SbPh₄(ECO), SbPh₄(MCO), SbPh₄(TDCO), and SbPh₄(TCO), and three control compounds, H(ACO), H(ECO), and H(MCO), were included. Dried discs with no material loaded were used as negative controls.

Bacterial strains and growth media. Low-salt Luria–Bertani (LB) medium was used for antimicrobial susceptibility testing. The bacterial stains included Gram-negative *Escherichia coli* strain S17(O113:H4) isolated from a chick liver with septicemia and lab-adapted burn-wound isolate *Pseudomonas aeruginosa* strain PAO1, and Gram-positive methicillin resistant *Staphylococcus aureus* strain NRS70. All strains were maintained in 10% skim milk at -80 °C. Before each experiment, the bacterial strains were inoculated onto LB agar from frozen stocks and grown overnight at 37 °C, from which isolated colonies were picked for inoculating LB broth and the subsequent testing.

Susceptibility testing for bacteria. Discs to be tested were prepared as described above. Bacterial cultures were grown in LB broth shaking at 200 rpm for 12 h at 37 °C. The optical density of the cultures at 600 nm (OD_{600 nm}) was measured and adjusted to 0.1 in LB broth, and 100 μ L of the cultures were spread on LB plates. The plates were allowed to dry for 10 min before impregnating filter paper discs containing test compounds using sterile forceps. As a control, 10 μ L of phosphate-buffered saline (PBS) was applied onto the discs. The plates were incubated at 37 °C for 24 h. Antibacterial activity was determined by measuring the clearance zones surrounding the discs. Considering irregular shapes of some clearances, three measurements for each sample were performed and averaged. Each experiment was conducted using three biological replicates, and the clearance zones were reported as the mean + standard error of the mean (SEM).

Fungal strains and growth media. *Cryptococcus neoformans* strain H99 (serotype A, mating type α) and *Candida albicans* strain SC5314 were recovered from 15% glycerol stocks

stored at $-80\text{ }^{\circ}\text{C}$ and were cultured on yeast extract–peptone–dextrose (YPD) plates (BD Difco; Franklin Lakes, NJ, USA).

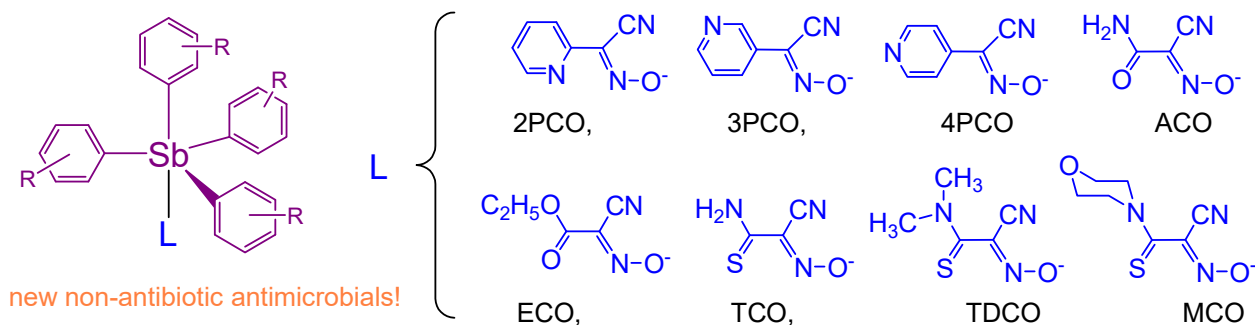
Susceptibility testing for fungi. Discs to be tested were prepared as described above. Fungal cultures were taken from YPD plates and grown in YPD broth shaking at 180 rpm for 18 h at $30\text{ }^{\circ}\text{C}$. Cells were centrifuged and washed $3\times$ with sterile PBS. Cells were quantified on a hemacytometer using trypan blue dye exclusion, and cultures were adjusted to 1×10^6 cells/mL in PBS. A volume of 100 μL of the culture was spread onto each YPD plate. The plates were allowed to dry for 10 min before placing filter paper discs containing test compounds using sterile forceps. A volume of 10 μL of PBS was applied to each disc to aid in diffusion. The plates were incubated at $30\text{ }^{\circ}\text{C}$ for 48 h. Antifungal activity was determined by measuring the clearance zones surrounding the discs. Three measurements for each sample were performed and averaged, and each experiment was conducted using three biological replicates. Clearance zones are reported as the mean \pm SEM.

4. Conclusions

For the first time, a series of novel organoantimony(V) cyanoximates with specially selected features was obtained and thoroughly studied in this interdisciplinary research aimed at a search for new non-antibiotic antimicrobials. As a summary of the conducted investigations, we report the following:

- (1) We designed high-yield synthesis of a series of eight novel tetraphenyl-antimony(V) cyanoximates of $\text{SbPh}_4(\text{L})$ composition using an effective and clean heterogeneous metathesis reaction involving solid silver(I) or thallium(I) compounds in acetonitrile solutions.
- (2) The prepared complexes represent crystalline white molecular solids (two compounds with thioamide-cyanoximes TCO^- and TDCO^- are yellow) well soluble in organic solvents.
- (3) All the synthesized compounds were characterized by ^1H - and ^{13}C -NMR, vibrational spectroscopy (IR and Raman), variable-temperature UV/visible spectroscopy, thermal analysis, and X-ray analysis.
- (4) Several correlations between pK_a values of starting cyanoxime and solid-state structures of $\text{SbPh}_4(\text{L})$ were determined (a) between off-plane Sb–O distance in trigonal bipyramids of compounds and (b) between Sb–O distances.
- (5) The crystal structures were determined for all eight new tetraphenyl-antimony(V) cyanoximates and show monodentate O-binding of the anion to the central atom.
- (6) All synthesized compounds were thermally stable in the solid state and in solutions up to $140\text{ }^{\circ}\text{C}$, which is an important property in light of their thermal sterilization for intended applications as topical antimicrobial agents added to coating and paints.
- (7) For the first time, a series of organometallic Sb-compounds of SbPh_4L composition were carefully designed for in vitro antimicrobial testing.
- (8) When tested for antibacterial potential, $\text{SbPh}_4(\text{ACO})$ and $\text{SbPh}_4(\text{ECO})$ showed activity against three selected bacterial pathogens, *E. coli*, *P. aeruginosa*, and *S. aureus*. known for their outstanding antibiotic resistance. $\text{SbPh}_4(\text{ACO})$, $\text{SbPh}_4(\text{ECO})$, and SbPh_4MCO showed a broad impact against the three bacteria, and $\text{SbPh}_4(\text{TDCO})$ was active only against Gram-positive *S. aureus*.
- (9) Antifungal studies showed that $\text{SbPh}_4(\text{MCO})$ was the only compound to inhibit the growth of both fungal pathogens *C. neoformans* and *C. albicans*, also known for their increasing resistance to antimicrobials. The other compounds inhibited the growth of *C. neoformans* but not *C. albicans*.

Table of content picture (General formula for the first series of new non-antibiotic antimicrobial compounds.):



Synopsis:

For the first time, a series of novel organoantimony(V) cyanoximates with specially selected features was obtained and thoroughly characterized using spectroscopic methods, as well as thermal and X-ray analyses. Compounds were found to be stable in the solid state and in solutions, representing new non-antibiotic compounds active against both pathogenic microorganisms and fungi.

Supplementary Materials: The following are available online at <https://www.mdpi.com/article/10.3390/molecules27217171/s1>: S1. Actual photographs of TIL (L = thioamide-cyanoximes) and results of elemental analysis; S2. Instrumentation and accessories for the isolation of SbPh₄L; S3. Details of synthesis of Tl(TCO) and its elemental composition; S4. Microscope photographs of crystals of SbPh₄L (L = thioamide-cyanoximes); S5. Table of IR frequencies of all SbPh₄L compounds; S6. Data of CNMR spectra of chemical shifts of phenyl-groups in SbPh₄L; S7, S8. Chemical shift values in the CNMR spectra of cyanoximes in SbPh₄L; S9–11. Actual ¹³C{¹H}-NMR spectra; S12, S13. Face-indexed single crystals of several compounds for proper absorption correction; S14–S22. Details of crystallographic characterization of synthesized organoantimony(V) compounds; S23. Example of TG/DSC traces of one of the compounds showing phase transition; S24. Correlations between pK_a values of cyanoximes and ¹³C chemical shift values; S25, S26. The clearance zones determined by the disc-diffusion assay; S27, S28. Representative images of discs in diffusion assay; S29. The checkCIF reports of all presented crystal structures.

Author Contributions: K.P. prepared and chemically characterized all studied compounds; N.G. initiated the project and provided its overall supervision; T.S. and O.M. performed antibacterial studies; M.A.P. directed the antibacterial studies and edited the manuscript; K.C. performed antifungal studies; K.L.W. directed the antifungal studies and edited the manuscript. All authors have read and agreed to the published version of the manuscript.

Funding: N.G. received partial funding from the MSU Graduate College as FRG; M.P.'s research was supported by the NIH P20GM103648 award; K.C. would like to thank the Lew Wentz Foundation and the Niblack Research Scholars program for partial support during this investigation.

Data Availability Statement: All results of this study and data from the Supporting Information are available to the public via the journal's portal.

Acknowledgments: N.G. is thankful to Sergiy Tyukhtenko (Northeastern University, Boston, MA) for his generous help with recording NMR spectra of several new organoantimonials at his research facility, and to Ilia Guzei (University of Wisconsin-Madison, WI) for high-intensity data collection for one of the compounds. K.P. would like to thank the MSU Graduate College for support during this investigation.

Conflicts of Interest: The authors declare no conflict of interest.

Sample Availability: Samples of the compounds might be available from the authors upon supply of SbPh₄Br (or chloride) from an interested party for the preparation of desired compounds.

References

1. Williams, K.J. The introduction of “chemotherapy” using arsphenamine—the first magic bullet. *J. R. Soc. Med.* **2009**, *102*, 343–348. [CrossRef] [PubMed]
2. Paul, N.P.; Galván, A.E.; Yoshinaga-Sakurai, K.; Rosen, B.P.; Yoshinaga, M. Arsenic in medicine: Past, present and future. *Biometals* **2022**, 1–19. [CrossRef] [PubMed]
3. The History of Pepto-Bismol. Available online: <https://pepto-bismol.com/en-us/article/the-history-of-pepto> (accessed on 1 August 2022).
4. Carmalt, C.; Norman, N. Arsenic, antimony and bismuth: Some general properties and aspects of periodicity. *Chem. Arsen. Antimony Bismuth* **1998**, 1–38.
5. Periferakis, A.; Caruntu, A.; Periferakis, A.-T.; Scheau, A.-E.; Badarau, I.A.; Caruntu, C.; Scheau, C. Availability, Toxicology and Medical Significance of Antimony. *Int. J. Environ. Res. Public Health* **2022**, *19*, 4669. [CrossRef]
6. Haldar, A.K.; Sen, P.; Roy, S. Use of antimony in the treatment of leishmaniasis: Current status and future directions. *Mol. Biol. Int.* **2011**, *2011*, 571242. [CrossRef]
7. Gasser, G.; Ott, I.; Metzler-Nolte, N. Organometallic anticancer compounds. *J. Med. Chem.* **2011**, *54*, 3–25. [CrossRef]
8. Frezard, F.; Demicheli, C.; Ribeiro, R.R. Pentavalent antimonials: New perspectives for old drugs. *Molecules* **2009**, *14*, 2317–2336. [CrossRef]
9. Agrawal, R.; Sharma, J.; Nandani, D.; Batra, A.; Singh, Y. Triphenylarsenic(V) and -antimony(V) derivatives of multidentate Schiff bases: Synthesis, characterization, and antimicrobial activities. *J. Coord. Chem.* **2011**, *64*, 554–563. [CrossRef]
10. Khan, N.U.; Sultana, D.; Nadeem, H. Synthesis, characterization, antibacterial activity of new antimony iii complexes of some tosyl-sulfonamide derivatives. *Middle East J. Sci. Res.* **2013**, *17*, 705–711.
11. Oliveira, L.G.; Silva, M.M.; Paula, F.C.; Pereira-Maia, E.C.; Donnici, C.L.; Simone, C.A.; Frezard, F.; Silva, E.N., Jr.; Demicheli, C. Antimony(V) and bismuth(V) complexes of lapachol: Synthesis, crystal structure and cytotoxic activity. *Molecules* **2011**, *16*, 10314–10323. [CrossRef]
12. Sharma, P.K.; Rehwani, H.; Rai, A.K.; Gupta, R.S.; Singh, Y.P. Antispermatic activity of the benzothiazoline ligand and corresponding organoantimony(V) derivative in male albino rats. *Bioinorg. Chem. Appl.* **2006**, *2006*, 16895. [CrossRef]
13. Singh, R.V.; Mahajan, K.; Swami, M.; Dawara, L. Microwave Assisted Synthesis, Spectroscopic Characterizations In-Vitro Antibacterial And Antifungal Properties Of Some Antimony And Bismuth Complexes Derived From NnO And NnS Donor Imines. *Main Group Met. Chem.* **2010**, *33*, 141–156. [CrossRef]
14. Gerasimchuk, N. Chemistry and Applications of Cyanoximes and Their Metal Complexes. *Dalton Trans.* **2019**, *48*, 7985–8013. [CrossRef] [PubMed]
15. Mokhir, A.A.; Domasevich, K.V.; Kent Dalley, N.; Kou, X.; Gerasimchuk, N.N.; Gerasimchuk, O.A. Syntheses, crystal structures and coordination compounds of some 2-hetarylcyanoximes. *Inorg. Chim. Acta* **1999**, *284*, 85–98. [CrossRef]
16. Gerasimchuk, N. An Excursion into the Intriguing World of Polymeric Tl(I) and Ag(I) Cyanoximates. *Polymers* **2011**, *3*, 1475–1511. [CrossRef]
17. Gerasimchuk, N. Synthesis, Properties, and Applications of Light-Insensitive Silver(I) Cyanoximates. *Eur. J. Inorg. Chem.* **2014**, *2014*, 4518–4531. [CrossRef]
18. Ciba Geigy, A.G. Srodek Ochrony Roslin Przed Dzialaniem Agresywnych Chemikalii Rolniczych. Poland Patent 127786, 1985.
19. Ciba Geigy, A.G. Mittel Zum Schutz Von Kulturpflanzen Von Agressiven Herbiziden. Patent of Austria 367268, 1982.
20. Davidson, S.H. 2-Cyano-2-Hydroximinoacetamides as Plant Disease Control Agents. U.S. Patent 3957847, 1978.
21. Skopenko, V.V.; Palii, G.K.; Gerasimchuk, N.N.; Makats, E.F.; Domashevskaya, O.A.; Rakovskaya, R.V.; Domasevitch, K. Nitrosothiocarbamylcyanmethanid of Potassium or Sodium Which Show Antimicrobial Activity. Patent of the USSR 1405281, 1988.
22. Lin, K. Process for Making 2-Cyano-2-Hydroximinoacetamide Salts. U.S. Patent 3919284, 1976.
23. Kuhne, A.; Hubele, A. Method for the Cultivation of Plants Employing R-Cyano Hydroximinoacetamide Derivatives. US Patent 4063921, 1978.
24. Domasevitch, K.V.; Gerasimchuk, N.N.; Mokhir, A. Organoantimony(V) cyanoximates: Synthesis, spectra and crystal structures. *Inorg. Chem.* **2000**, *39*, 1227–1237. [CrossRef]
25. Eddings, D.; Barnes, C.; Gerasimchuk, N.; Durham, P.; Domasevich, K. First bivalent palladium and platinum cyanoximates: Synthesis, characterization, and biological activity. *Inorg. Chem.* **2004**, *43*, 3894–3909. [CrossRef]
26. Gerasimchuk, N.; Maher, T.; Durham, P.; Domasevitch, K.V.; Wilking, J.; Mokhir, A. Tin(IV) cyanoximates: Synthesis, characterization, and cytotoxicity. *Inorg. Chem.* **2007**, *46*, 7268–7284. [CrossRef]
27. Mann, A.; Gerasimchuk, N.; Silchenko, S. New non-aggregating bivalent cis-ML₂ (M = Pd, Pt; L = pivaloylcyanoxime). *Inorg. Chim. Acta* **2016**, *440*, 118–128. [CrossRef]
28. Domasevitch, K.V.; Skopenko, V.V.; Rusanov, E.B. Synthesis, Infrared and X-ray Studies of Diphenyltellurium(IV) Nitrosocarbamylcyanmethanides. X-Ray Evidence for Stability of a Tritelluroxane Fragment -Ph₂Te-O-Ph₂Te-O-Ph₂Te. *Z. Nat. B* **1996**, *51*, 832–837. [CrossRef]
29. Mokhir, A.A.; Gerasimchuk, N.N.; Pol’shin, E.V.; Domasevitch, K.V. Synthesis, IR and Mossbauer study of bisorganotin complexes with cyanoximes. *Russ. J. Inorg. Chem.* **1994**, *39*, 289–293.

30. Riddles, C.N.; Whited, M.; Lotlikar, S.R.; Still, K.; Patrauchan, M.; Silchenko, S.; Gerasimchuk, N. Synthesis and Characterization of Two Cyanoxime Ligands, Their Precursors, and Light Insensitive Antimicrobial Silver(I) Cyanoximates. *Inorg. Chim. Acta* **2014**, *412*, 94–103. [[CrossRef](#)]
31. Gerasimchuk, N. Synthesis, Characterization and Remarkable Applications of Light-insensitive Silver(I) Cyanoximates. *New Trends Coord. Bioinorg. Appl. Inorg. Chem.* **2011**, 106–113.
32. Glover, G.; Gerasimchuk, N.; Biagioni, R.; Domasevitch, K.V. Monovalent K, Cs, Tl, and Ag nitrosodicyanomethanides: Completely different 3D networks with useful properties of luminescent materials and nonelectric sensors for gases. *Inorg. Chem.* **2009**, *48*, 2371–2382. [[CrossRef](#)] [[PubMed](#)]
33. Gerasimchuk, N.N.; Tchernega, A.N.; Kapshuk, A.A. Synthesis, IR spectra and structure of complex Tl(I) with carbamoyl-cyanoxime HONC(CN)C(O)NH₂. *Russ. J. Inorg. Chem.* **1993**, *38*, 1530–1534.
34. Marcano, D.; Gerasimchuk, N.; Nemykin, V.; Silchenko, S. Synthesis, Characterization, and Studies of Coordination-Polymeres With Isomeric Pyridylcyanoximes: Route to Metal Ribbons With Very Short Tl···Tl Separations. *Cryst. Growth Des.* **2012**, *12*, 2877–2889. [[CrossRef](#)]
35. Curtis, S.; Lottes, B.; Robertson, D.; Lindeman, S.V.; Gerasimchuk, N. Search for the shortest intermetallic Tl—Tl contacts: Synthesis and characterization of Thallium(I) coordination polymers with several mono- and bis-cyanoximes. *Inorg. Chim. Acta* **2020**, *508*, 119597. [[CrossRef](#)]
36. Morton, J.; Dennison, R.; Nemykin, V.; Gerasimchuk, N. Planochromism of cyanoxime anions: Computational and mechanistic studies in solid state and solutions. *Inorg. Chim. Acta* **2020**, *507*, 119570. [[CrossRef](#)]
37. Rojas, T.C.G.; Maluta, R.P.; Parizzi, L.P.; Koenigkan, L.V.; Yang, J.; Yu, J.; Pereira, G.A.G.; Dias da Silveira, W.J.G.A. Genome sequences of avian pathogenic Escherichia coli strains isolated from Brazilian commercial poultry. *Genome Announc.* **2013**, *1*, e00110-13. [[CrossRef](#)]
38. Stover, C.K.; Pham, X.Q.; Erwin, A.L.; Mizoguchi, S.D.; Warren, P.; Hickey, M.J.; Brinkman, F.S.; Hufnagle, W.O.; Kowalik, D.J.; Lagrou, M.; et al. Complete genome sequence of Pseudomonas aeruginosa PA01, an opportunistic pathogen. *Nature* **2000**, *406*, 959–964. [[CrossRef](#)] [[PubMed](#)]
39. Kuroda, M.; Ohta, T.; Uchiyama, I.; Baba, T.; Yuzawa, H.; Kobayashi, I.; Cui, L.; Oguchi, A.; Aoki, K.; Nagai, Y.; et al. Whole genome sequencing of meticillin-resistant Staphylococcus aureus. *Lancet* **2001**, *357*, 1225–1240. [[CrossRef](#)]
40. Harmsen, M.; Yang, L.A.; Pamp, S.J.; Tolker-Nielsen, T. An update on Pseudomonas aeruginosa biofilm formation, tolerance, and dispersal. *Fems. Immunol. Med. Mic.* **2010**, *59*, 253–268. [[CrossRef](#)] [[PubMed](#)]
41. Haaber, J.; Penades, J.R.; Ingmer, H. Transfer of Antibiotic Resistance in Staphylococcus aureus. *Trends Microbiol.* **2017**, *25*, 893–905. [[CrossRef](#)] [[PubMed](#)]
42. Bernier, S.P.; Surette, M.G. Concentration-dependent activity of antibiotics in natural environments. *Front. Microbiol.* **2013**, *4*, 20. [[CrossRef](#)] [[PubMed](#)]
43. Sanglard, D.; Coste, A.; Ferrari, S. Antifungal drug resistance mechanisms in fungal pathogens from the perspective of transcriptional gene regulation. *FEMS Yeast Res.* **2009**, *9*, 1029–1050. [[CrossRef](#)]
44. Smith, K.D.; Achan, B.; Hullsiek, K.H.; McDonald, T.R.; Okagaki, L.H.; Alhadab, A.A.; Akampurira, A.; Rhein, J.R.; Meya, D.B.; Boulware, D.R.; et al. Increased Antifungal Drug Resistance in Clinical Isolates of Cryptococcus neoformans in Uganda. *Antimicrob. Agents Chemother.* **2015**, *59*, 7197–7204. [[CrossRef](#)]
45. Chang, M.; Sionov, E.; Khanal Lamichhane, A.; Kwon-Chung, K.J.; Chang, Y.C. Roles of Three Cryptococcus neoformans and Cryptococcus gattii Efflux Pump-Coding Genes in Response to Drug Treatment. *Antimicrob. Agents Chemother.* **2018**, *62*, e01751-17. [[CrossRef](#)]
46. Gerasimchuk, N.N.; Domasevitch, K.V.; Kapshuk, A.A. Coordination compounds of N,N-dimethylthioamidocyanoxime. *Russ. J. Inorg. Chem.* **1993**, *38*, 1718–1722.
47. Conrad, M.; Schulze, A. Isonitrosocyanessigsäure ätyl ester. *Berichte* **1909**, *42*, 745.
48. Gerasimchuk, N.; Gamian, A.; Glover, G.; Szponar, B. Light Insensitive Silver(I) Cyanoximates As Antimicrobial Agents for Indwelling Medical Devices. *Inorg. Chem.* **2010**, *49*, 9863–9874. [[CrossRef](#)] [[PubMed](#)]
49. Emsley, J. *The Elements*; Clarendon Press: Oxford, UK, 1991.
50. Glaser, J. *Advances in Inorganic Chemistry*; Sykes, A.J., Ed.; Academic Press: San Diego, CA, USA, 1995; Volume 43, p. 1.
51. Heydlauf, H. Ferric-cyanoferrate (II): An effective antidote in thallium poisoning. *Eur. J. Pharm.* **1969**, *6*, 340–344. [[CrossRef](#)]
52. Sheldrick, G. *SHELXTL*, Version 2014/7. 2014.
53. Farrugia, L. ORTEP-3 for Windows—a version of ORTEP-III with a Graphical User Interface (GUI). *J. Appl. Crystallogr.* **1997**, *30*, 565. [[CrossRef](#)]
54. Gerasimchuk, N.; Esaulenko, A.N.; Dalley, K.N.; Moore, C. 2-Cyano-2-isonitrosoacetamide and its Ag(i) complexes. Silver(i) cyanoximate as a non-electric gas sensor. *Dalton Trans.* **2010**, *39*, 749–764. [[CrossRef](#)] [[PubMed](#)]